Proceedings of the Indian National Science Academy (2024) 90:982–996
https://doi.org/10.1007/s43538-024-00287-w

RESEARCH PAPER

Geophysical and geochemical studies on sinking stream occurrence in Ayankulam village of South Tamilnadu, India

A. Antony Ravindran[1] · A. Antony Alosanai Promilton[1,2] · J. Vinoth Kingston[1] · S. Richard Abishek[1] · S. K. Aswin[1] · R. Abinaya[1] · R. Sakthi Priya[1]

Received: 8 November 2023 / Accepted: 24 March 2024 / Published online: 30 April 2024

Abstract

The severe monsoon flooding in 2021 exposed the intricate hydrogeological processes affecting groundwater resources near Ayankulam village in the semi-arid terrain of South Tamil Nadu, India. Despite extensive inundation from overflow of the Nambiar canal, the village well remained dry due to diversion of recharge away from shallow aquifers into deeper concealed karst formations present in the underlying calcarenite bedrock. Detailed geophysical surveys utilizing Azimuthal Square array resistivity combined with Magnetotellurics successfully identified and mapped subsurface pathways of sinking streams that rapidly transported surface water vertically into deeper fractured basement aquifers instead of laterally recharging the shallower dug well. Geochemical analysis of groundwater samples collected from wells in the area revealed progressive evolution of ionic compositions along groundwater flow paths dominated by water–rock interactions including carbonate mineral dissolution, silicate weathering, cation exchange and evaporation. Findings indicated that excessive recharge from heavy rainfall events caused accelerated subsurface drainage of fresh groundwater away from inland recharge zones near Ayankulam village towards the coast. This rapid drainage driven by the hydrostatic pressure exerted by the intense monsoon recharge on the highly permeable karst conduit networks buried beneath the low permeability overlying clay-rich soils. The diversion of freshly recharged water from the surface into deeper aquifers before it could reach the shallow dug well resulted in the phenomenon of "dry fallout" observed in Ayankulam village. This integrated geophysical and geochemical study provided evidence that sinking streams and the complex linkage between shallow and deeper aquifers control groundwater occurrence and movement in the region. The findings emphasize the need for enhanced monitoring and measurement of hydrogeological parameters coupled with integrated water resources management. This is vital for sustainably harnessing water resources amidst growing demands from the increasing population and intensifying climate change pressures that exacerbate rainfall variability.

Keywords Sinking Stream · Karst Formation · Intricate · Calcarenite rock and Dry fall out

Introduction

Groundwater is a vital resource for both human needs and ecosystem health, and sinking streams are one of its key sources (Goldscheider 2019). Groundwater and sinking streams are both components of the water cycle, but they differ in their physical properties and movement (White 2002; Goldscheider 2019). Groundwater is the water that saturates the pores and fractures in geologic formations beneath the land surface, flowing slowly through the subsurface and eventually discharging into streams, rivers, and other surface water bodies (Bowen 1986). In contrast, sinking streams, also known as losing streams, are surface water bodies that flow into the ground and recharge the groundwater aquifer (Bonacci 2015). The water in sinking streams moves quickly through the subsurface, typically in areas with karst geology, and can emerge in springs or wells in other locations (Barry et al. 2018). While both groundwater and sinking streams contribute to the water cycle, they differ in their flow rates, movement, and interaction with the land surface (Katz et al.

✉ A. Antony Ravindran
antonicogeo@gmail.com

[1] PG and Research Department of Geology, V.O.Chidambaram College, Thoothukudi, Tamilnadu, India

[2] (Reg. No: 19212232221033) Research Scholar Manonmaniam Sundaranar University, Tirunelveli, Tamilnadu, India

1998). Exploring these water resources in arid and semi-arid regions can present formidable challenges, but geophysical methods offer a vital means of continuously scanning and evaluating subsurface water saturation—a crucial task, particularly in remote areas (Ravindran 2012; Sener et al. 2021).

Geophysical methods, such as electrical resistivity method, ground-penetrating radar (GPR), and electromagnetic (EM) surveys used to map the subsurface geology, identify areas with high water content, and detect the presence of sinkholes or other features associated with sinking streams (Gomo 2023). Square array resistivity method and magnetotelluric (MT) are two geophysical techniques used for identifying sinking streams (Ravindran 2012; Nenna et al. 2013). The square array resistivity method is particularly useful in areas with shallow water tables, as it can provide high-resolution images of the subsurface (Obiadi et al. 2013). Magnetotelluric method can provide information on the electrical conductivity of the subsurface at different depths and made comparison of both methods regarding the subsurface changes in formation as well as groundwater location (Gomo 2023). Both techniques used to map the subsurface geology, identify areas with high water content, and detect the presence of sinkholes or other features associated with sinking streams. However, the quality of the presence of the water present beneath the earth surface varies due to different conditions, which can be associated by geochemical approach (Ravindran 2012; Obiadi et al. 2013; Sener et al. 2021).

The use of geochemistry for identifying sinking streams is essential for understanding the complex chemical and physical interactions between water, rock, and soil in the subsurface (Krishna Kumar et al. 2014). Sinking streams are unique features in karst landscapes where surface water infiltrates into the subsurface through sinkholes or other types of conduits, recharging groundwater aquifers (Barry et al. 2018; Jeelani et al. 2011). Geochemistry provides valuable insights into the movement and interaction of water, solutes, and gases in the subsurface, which is crucial for identifying sinking streams and their connection to groundwater (Katz et al. 1998). Analysing the chemical composition of groundwater and surface water can identify the sources and pathways of water flow, track the movement of solutes and contaminants, and detect changes in water quality that may indicate the presence of sinking streams (Ammar 2015). The use of geochemistry in identifying sinking streams and their connection to groundwater is essential for developing a comprehensive understanding of the complex hydrological systems in karst areas (Katz et al. 1998; Goldscheider 2019).

There are very limited researches carried for the sinking streams occurrences and their impact to the surrounding environment. The article by Barry et al. (2018) provides an innovative and comprehensive approach to understanding the hydrologic system of a siliciclastic pseudo-karst aquifer in southeast Minnesota, USA, using a combination of dye tracing, water chemistry, and passive geophysics. Jeelani et al. (2011) presents a thorough geochemical analysis of surface water and spring water in the SE Kashmir Valley, Western Himalaya, providing valuable insights into water–rock interaction and hydro-geochemical processes in the region associated with sinking streams. Zhu et al. (2011) highlights the challenges of using electrical resistivity methods to locate karst conduits in the Inner Bluegrass Region, Kentucky, and provides useful insights for improving the accuracy and reliability of geophysical surveys in karst terrains. Kaufmann and Romanov (2016) provides a comprehensive analysis of the structure and evolution of collapse sinkholes through the integration of physico-chemical modeling and geophysical fieldwork, highlighting the importance of understanding the complex processes that contribute to their formation. The study by Martel et al. (2018) demonstrates the combined use of electrical resistivity tomography, ground penetrating radar, interferometric synthetic aperture radar, and tracer tests to effectively characterize and visualize complex karst aquifer systems beneath urban areas without drilling or disruption, as exemplified in their research on the karstic groundwater underlying Quebec City. During periods of flooding or low water availability, the physical interactions between sinking streams and the movement of groundwater within the karst aquifer become crucial factors to consider. The ponor zone serves as a conduit for sinking streams, allowing them to merge with the potentiometric surface, thereby creating a dynamic relationship between these two elements (Koit et al. 2022; Bailly-Comte et al. 2010).

The overarching objectives of this research are threefold: firstly, to delineate and map subsurface fracture zones and associated sinking stream conduits within the predominant karst topography through implementation of geophysical techniques including azimuthal square array electrical resistivity surveying and magnetotelluric soundings; secondly, to analyze and interpret geochemical signatures of groundwater samples collected from selected wells across the study area in order to identify hydro-geochemical connections and flow pathways linking groundwater to the mapped sinking streams; and thirdly, to integrate the acquired geophysical and geochemical datasets to demonstrate and elucidate linkages between the delineated sinking stream networks and submarine groundwater discharge observed in the coastal zone, thereby facilitating conceptualization of the key occurrence mechanisms, pathways, and integral hydrological role of sinking streams in the complex subsurface hydraulic regime of the region.

Study area

The study area under examination is located in the coastal zone and encompasses diverse geological formations. Spanning the coordinates N 8°18.114′, E 77°51.086′ within the Tirunelveli district of Tamil Nadu, this region encompasses various soil types, including clay-rich soil, alluvium deposits, sandstone, Calcarenite, Leptinite, weathered gneissic rock, and basement rock (Fig. 1). The surface layer is typically covered by alluvium deposits throughout the entire region. The area experiences a subtropical climate, characterized by hot and dry conditions during May and June, and pleasantly cool weather in December and January. Humidity levels range from 79 to 84%, while the average minimum and maximum temperatures hover around 22.9 °C and 33.5 °C, respectively.

Rainfall

Data collected from IMD stations spanning 2010–2020 for the district. The semi-arid study area of Tirunelveli exhibits a highly seasonal rainfall regime dominated by the Northeast monsoon, with average October-December precipitation ranging from 138.9 to 193.7 mm. Extreme rainfall events over 300 mm frequently occur during this three-month period. Conversely, the region experiences considerably drier and more variable conditions during the Southwest monsoon (average rainfall of 20.6–38.6 mm over June–September). Over the past decade (2011–2020), the rainfall pattern shows high inter-annual variability, fluctuating between flood years with ample precipitation to drought years with severely deficient rainfall (IMD data). This point to growing rainfall erraticism, likely linked to changing monsoon dynamics and increasing climate change pressures in the region.

Geological and hydrogeological settings

The study area underlain predominantly by hard rock geological formations comprising charnockite and garnetiferous gneisses. The weathered zones in these formations extending up to depths of 10–35 m below ground level form potential aquifers. Aquifer parameters indicate moderate groundwater potential in the district, with specific capacity ranging from 12 to 78 lpm/m-d, transmissivity varying from 3 to 212 m^2/d, and yields of dug wells being 0.15–6 lps. Pre-monsoon water levels range between ground level and 15 m below ground level (CGWB). However, post-monsoon water levels rise

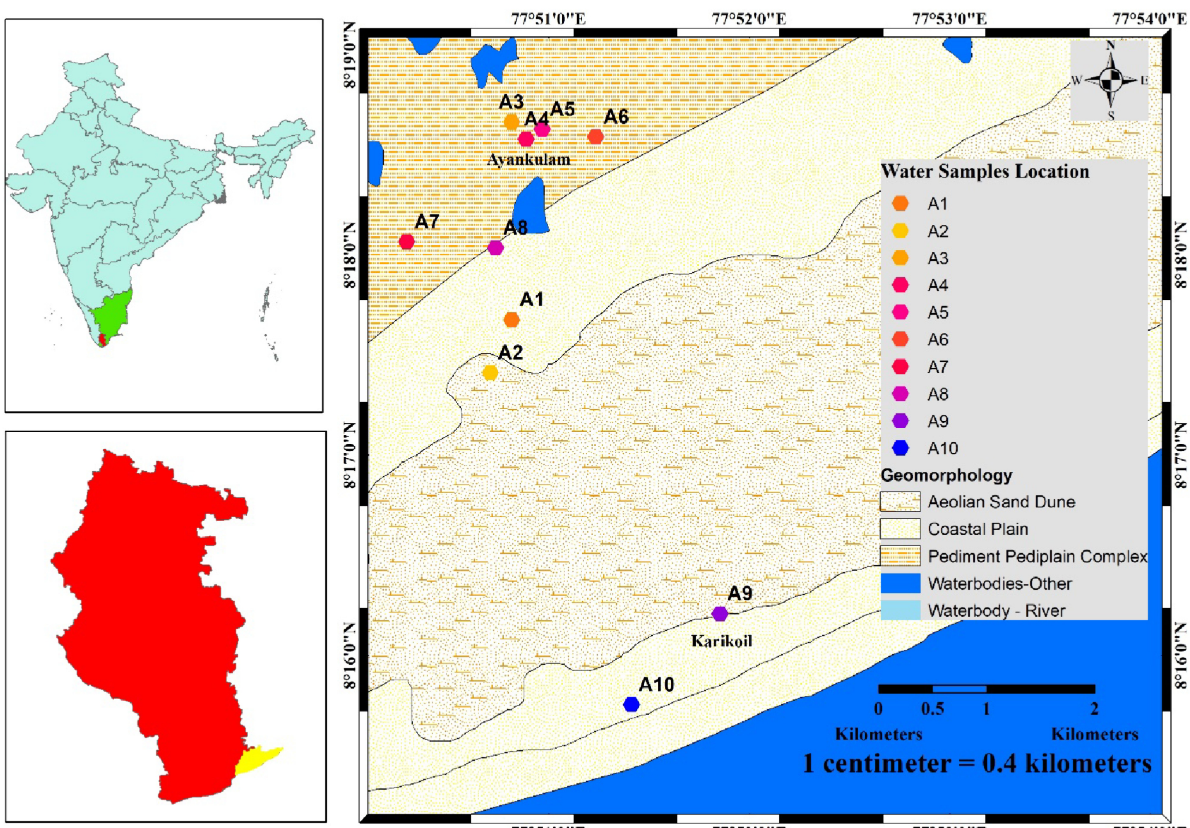

Fig. 1 Study Area map showing collected water sample location and Geomorphology

due to recharge and may even reach ground level. Long term analysis of groundwater level data indicates declining trends in some parts of the district. The monitoring network comprises 168 observation wells and 82 piezometers but faces constraints like insufficient density, lack of alternate wells when existing ones fail, and outdated measurement equipment. Based on the 2013 assessment, the district categorized as Semi-Critical, with a 74% stage of groundwater development. While the overall water quality ranges from moderate to good, issues like salinity intrusion in coastal areas as per CGWB report.

Materials and methods

To investigate the presence of sinking stream groundwater, fractured zones, subsurface lithology, and groundwater flow channels in this study, a combination of geophysical and geochemical techniques was employed. Specifically, the Azimuthal square array approach, Magnetotelluric method, and Hydrogeochemistry method were utilized to conduct the exploration within the study area.

Azimuthal square array method

Geophysical techniques play a crucial role in indirectly mapping subsurface rock formations and identifying groundwater-related issues (Ramanujam et al. 2006). The implementation of azimuthal square arrays for resistivity studies proves particularly beneficial in detecting water-bearing formations and determining key parameters such as the depth, thickness, and extent of the water table (Habberjam 1972; Ramanujam et al. 2006). This information holds immense value in terms of anticipating future industrial development. By rotating an electrode array, it becomes possible to assess the directional variations in electrical anisotropy and calculate the apparent resistivity across different orientations (Habberjam 1972). The resistivity of soils and rocks influenced by the amount and quality of water present within their pore spaces and fractures (Habberjam 1972; Lane et al. 1995).

In the Azimuthal square array method, a square arrangement formed by inserting four electrodes into the ground. Three measurements taken for each square: two perpendicular measurements (α and β) were used to determine the apparent resistivity (ρa), while one diagonal measurement (γ) was performed to validate the results. In a homogeneous isotropic material, $\rho a\gamma$ would be equal to zero, while in a homogeneous anisotropic material, $\rho a\gamma$ would be equal to $\rho a\alpha - \rho a\beta$. The calculation of apparent resistivity followed the equation outlined in the research conducted by Habberjam and Watkins in 1967.

$$\rho a = K(\Delta V/I) \tag{1}$$

where, $K = 2\pi\ a/\ (2 - \sqrt{2})$ and "a" is the length of the side of a square array (Fig. 2).

To measure azimuthal apparent resistivity in this study, a square array utilized, with rotation around its center and expanded electrode spacing by a factor of $a\sqrt{2}$ at each azimuth. This approach allowed for the interpretation of resistivity data as an indicator of depth, which is crucial for detecting water-bearing formations and estimating their thickness and water table depth. In a homogeneous, isotropic material, the side length of the square array was approximately equal to the penetration depth. Data collection performed using the CRM-500 Aquameter instrument, consisting of a resistivity meter, steel electrodes, and a 12 Volts D.C. battery. Each cable set included four electrode cables, and the center point of the square array used to identify the measurement location.

Magnetotelluric method

The magnetotelluric method served as a valuable tool for investigating subterranean aquifers and associated geological features (Vozoff 1991; Falgàs et al. 2009). This technique enabled researchers to study landscape tectonic movements, freshwater migration, saline intrusion, aquifer thickness, and the transformation of river and coastal silt into meta-sedimentary rock from a geomorphological perspective (Abdelzaher et al. 2011). Previous studies have successfully employed magnetotelluric approaches to locate and characterize subsurface freshwater discharge, formations, and geology (Li and Jie 2017; Vozoff 1991; Abdelzaher et al. 2011; Falgàs et al. 2009; Demirci et al. 2017). The ADMT-300S equipment, equipped with M and N copper probes, used to perform the technique. The electrodes positioned at equal distances and depths of coverage to reach a depth of 300 m. Variation in resistivity allowed discrimination among different soil types, rocks, and shoreline boundaries. Magnetotelluric data collected from the M and N electrodes analyzed using Surfer software, which produced 2D and 3D models of subsurface rock structures.

Hydrogeochemistry

Groundwater is a dynamic system influenced by various factors, including host rock features and underlying rock types. Understanding the geochemical quality of groundwater is crucial for effective resource management for drinking, household and industrial purposes, as well as irrigation (Aris et al. 2007; Khan and Jhariya 2018; Krishna Kumar et al. 2014; Mostafa et al. 2017; Nagaraju et al. 2016). Sampling and analysis of

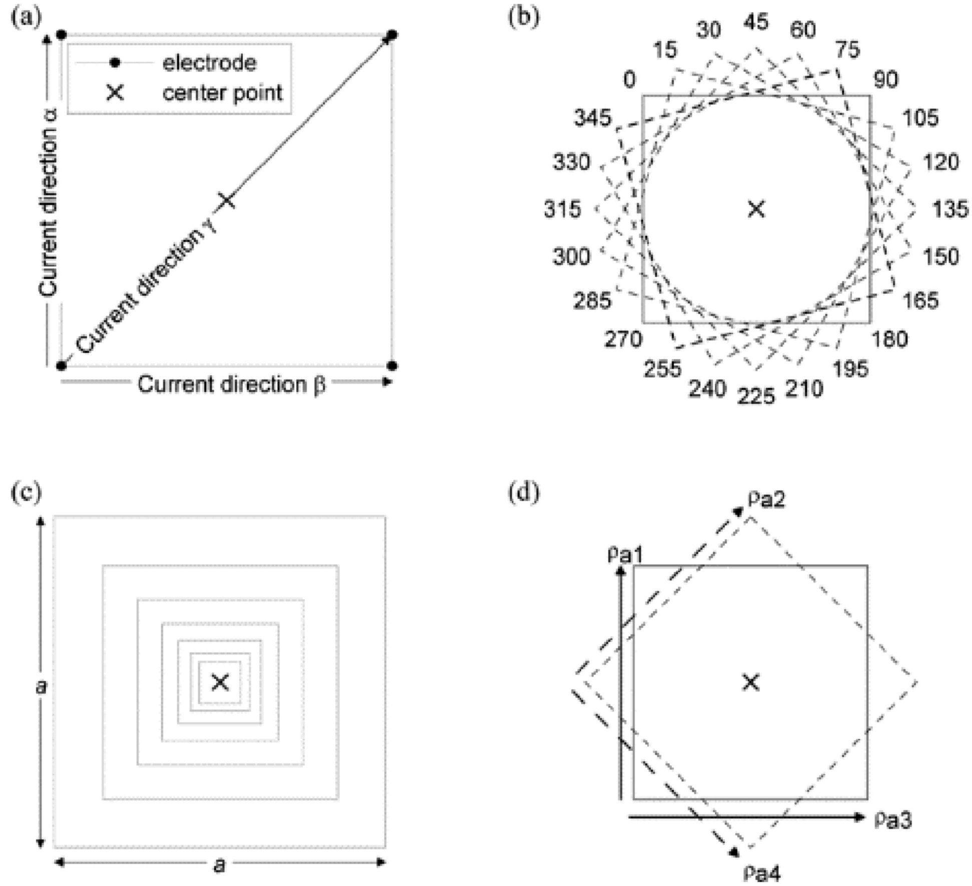

Fig. 2 Electrode configuration for data collection

groundwater from different locations are essential to evaluate its quality. One-litre polythene bottles used to collect samples, which rinsed with the sampled water to prevent contamination. Representative sampling ensured by pumping the well for a few minutes before collecting the sample. The collected data analyzed using various techniques, such as the Piper Trilinear Diagram and Wilcox Plot.

Parameters such as color, turbidity, total dissolved solids (TDS), electrical conductivity, pH, salinity, alkalinity, major cation, and anion concentrations were determined. The Piper Plot used to determine the percentage concentration of major cations and anions, while the Wilcox plot was useful for evaluating the suitability of irrigation water based on Na percentage and electrical conductivity (EC). Electrical conductivity commonly used to determine the salinity level of irrigation water, and Na percentage served as an essential indicator of water suitability for irrigation purposes.

Results and Discussion

Azimuthal square array

In this study, eight resistivity profiles collected in a NE-SW orientation utilizing the azimuthal square array method to delineate the subsurface geological structures and groundwater resources. Depth sounding curves generated for all profiles plotting the apparent resistivity values against the current electrode spacing, also referred to as the 'A' spacing. Analysis of the apparent resistivity-A spacing curves provides insights into the true resistivity and depth of the geological layers underlying each station (Ravindran 2012; Obiadi et al. 2013). The maximum recorded apparent resistivity value of 13,346 Ohm-m within the survey area is strongly indicative of the presence of crystalline basement rocks of the charnockite type at depth (Lane et al. 1995).

The results showed that in all the resistivity profiles collected, spanning depths of 25–40 m, freshwater saturated zones exhibiting relatively low resistivity values within the range of 100–120 Ohm-m were consistently detected at depths between 12 to 18 m. As resistivity inversely correlated to moisture content, these anomalous low resistivity zones interpreted to represent groundwater aquifers contained within saturated weathered/fractured basement bedrock (Yeboah-Forson and Whitman 2013; Sener et al. 2021). In profile 1, which covered a subsurface distance of 40 m in the NE-SW orientation, a prominent low resistivity anomaly indicative of a saturated freshwater zone was uncovered at depths of 8–10 m, exhibiting resistivity values of 100–120 Ohm-m. This likely represents water saturation within shallow fractured basement aquifers. Similarly, profile 2 reaching a depth of 30 m revealed a freshwater saturated zone at 12–14 m depth with resistivity of 100–120 Ohm-m, while profile 3 extending to 38 m depth uncovered a low resistivity anomaly at 13–16 m depth (100–120 Ohm-m) associated with fractured bedrock aquifers. Profile 4 imaged the subsurface up to 30 m depth and detected a freshwater zone at 13–14 m depth (100–120 Ohm-m). The depth versus apparent resistivity results for profiles 1 to 4 displayed in Fig. 3.

Furthermore, analysis of profiles 5 to 8 covering depths of 28 to 30 m consistently revealed low resistivity anomalies at 13–19 m depth, with resistivity ranging from 100 to 120 Ohm-m (Fig. 4). These zones interpreted to represent productive water-bearing weathered basement aquifers recharged by sinking stream deposits within the overlying formations (Ravindran 2012; Yeboah-Forson and Whitman 2013). Inverted 2D resistivity models revealed a layered sequence of topsoil, weathered/fractured gneiss at 5–12 m depth, freshwater-saturated calcarenite/leptinite beds at 12–22 m, gneissic/migmatite rock at 22–34 m, and basement charnockite below 34 m (Table 1). This agrees with typical stratification patterns in crystalline basement aquifer systems (Ramanujam et al. 2006, Ravindran 2012; Yeboah-Forson and Whitman 2013).

Magnetotelluric method

Magnetotelluric (MT) profiling of the study area includes six profiles, reaching depths of 100–300 m, revealed low resistivity anomalies (0.02–0.18 Ωm) indicative of saturated zones at 30–150 m depth (Fig. 5). As MT resistivities are inversely correlated with fluid saturation (Albouy et al. 2001; Li et al. 2017), these conductive zones likely represent sinking stream recharge into permeable weathered/fractured basement aquifers (Falgàs et al. 2009; Koit et al. 2022). Profile 1 exhibited a low resistivity anomaly (0.02–0.10 Ωm) at 30 m depth, while Profile 2 showed a conductive zone (0.048–0.07 Ωm) at 10 m depth. Profiles 3 and 4 detected a prominent saturated layer (0.10–0.18 Ωm) at 150 m depth. Resistivity models uncovered stratified lithology comprising near surface weathered rock (0.22–0.30 Ωm), underlain by water-bearing weathered/fractured gneissic bedrock. This agrees with typical crystalline basement stratification where surface clay-rich sinking stream deposits facilitate groundwater movement through deeper conduits in fractured basement rock (Falgàs et al. 2009; Bailly-Comte et al. 2010).

Profile 5 spans to a depth of 100 m over 24 m distance indicated near-surface weathered calcareous rock exhibiting resistivity values of 0.050–0.065 Ohm-m, underlain by fresh crystalline gneissic and granitic basement rock with higher resistivity in the range of 0.070–0.076 Ohm-m. The resistivity models are consistent with the typical subsurface stratification of deeply weathered terrains comprising clay-rich sinking stream deposits in the near surface underlain by fractured aquifers in the weathered bedrock overlying fresh and unweathered crystalline basement rock (Falgàs et al. 2009; Bailly-Comte et al. 2010). Profile 6 reached 300 m depth across 160 m distance revealed a prominent shallow low resistivity anomaly ranging from 0.047 to 0.067 Ohm-m occurring at a depth of around 150 m. This conductive zone interpreted to represent a significant fractured and weathered bedrock aquifer, likely saturated by the downward percolation of surface water from sinking stream deposits (Li et al. 2017; Gomo 2023).

Hydrogeochemistry

The water quality analysis of 10 samples collected from various sampling stations (A1 to A9) in and around Ayankulam village and (A9 and A10) in Karikovil and Uvari for different physio-chemical parameters including pH, temperature, electrical conductivity, total dissolved solids, major cations (sodium, potassium, magnesium, calcium), major anions (chloride, sulphate, bicarbonate, carbonate).

The pH values range from 6.81 to 9.66, indicating slightly acidic to slightly alkaline water. pH depends on geology, residence time and geochemical reactions (Glynn and Plummer 2005). The observed range reflects mixed influence of natural and anthropogenic factors. Temperature varies from 25 to 29.7 °C, which is normal groundwater temperature range, indicating recent recharge (Chou 2021). Electrical conductivity varies widely from 255 to 1070 µS/cm across samples. The total dissolved solids ranges from 170 to 705 mg/L. As per classification, the samples range from fresh (< 1000 mg/L TDS) to brackish (1000–10,000 mg/L TDS) type. The major cations in order of abundance are – calcium (11–79 mg/L), sodium (18–94 mg/L), magnesium (4–23 mg/L) and potassium (2–10 mg/L). The abundance indicates silicate mineral

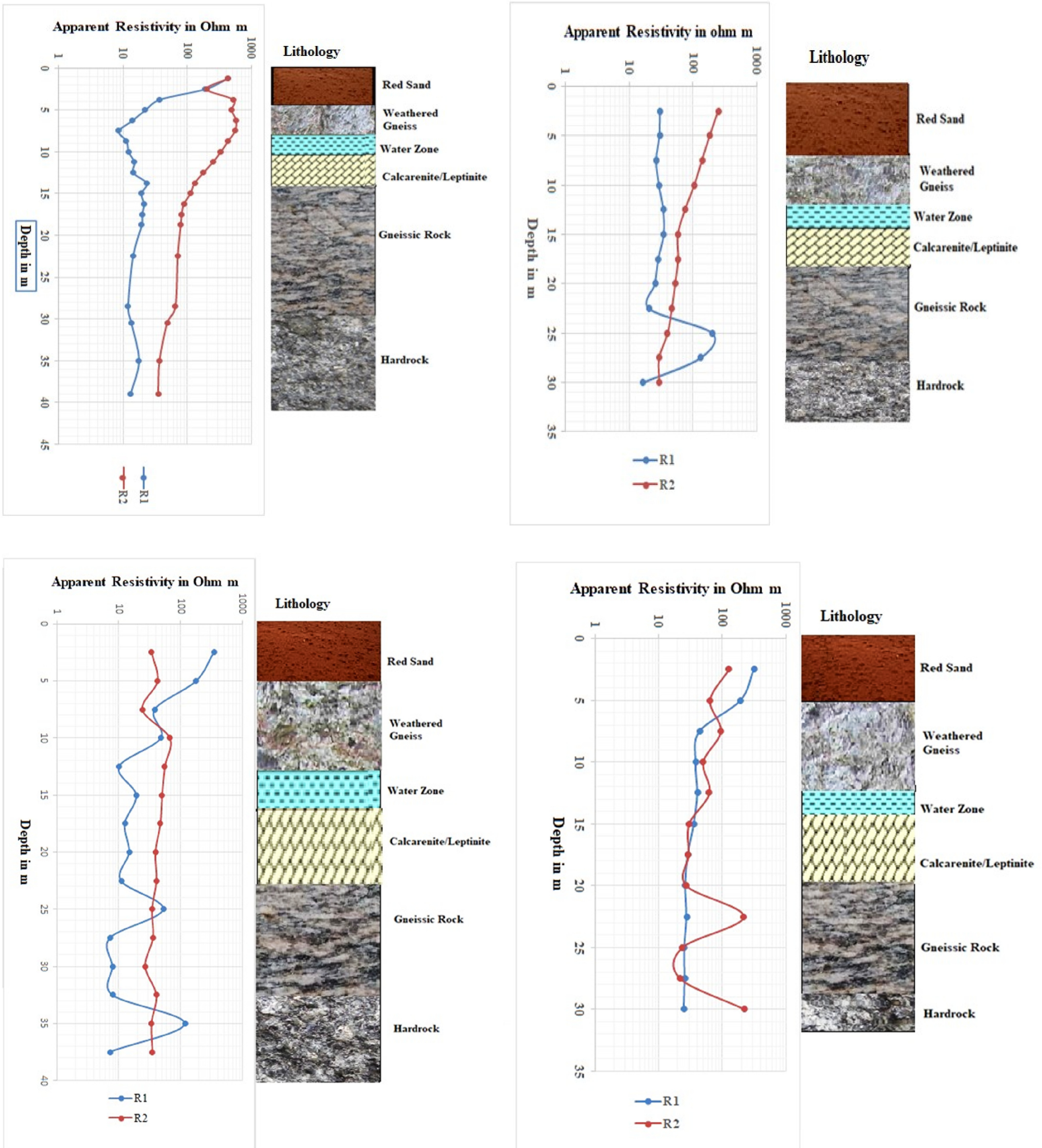

Fig. 3 Electrical resistivity profile 1 to 4

weathering influences the Ca-Mg composition while Na may come from evaporation and base exchange processes (Xiao et al. 2015). The major anions are bicarbonate (46–295 mg/L), chloride (31–141 mg/L) and sulphate (7–67 mg/L). Bicarbonate represents dissolved carbon dioxide from soil zone reactions. Chloride may be from natural or anthropogenic sources while sulphate comes from oxidation of sulphide minerals (Miao et al. 2013). The samples are slightly alkaline, fresh to brackish type, moderately hard water with mixed composition of major

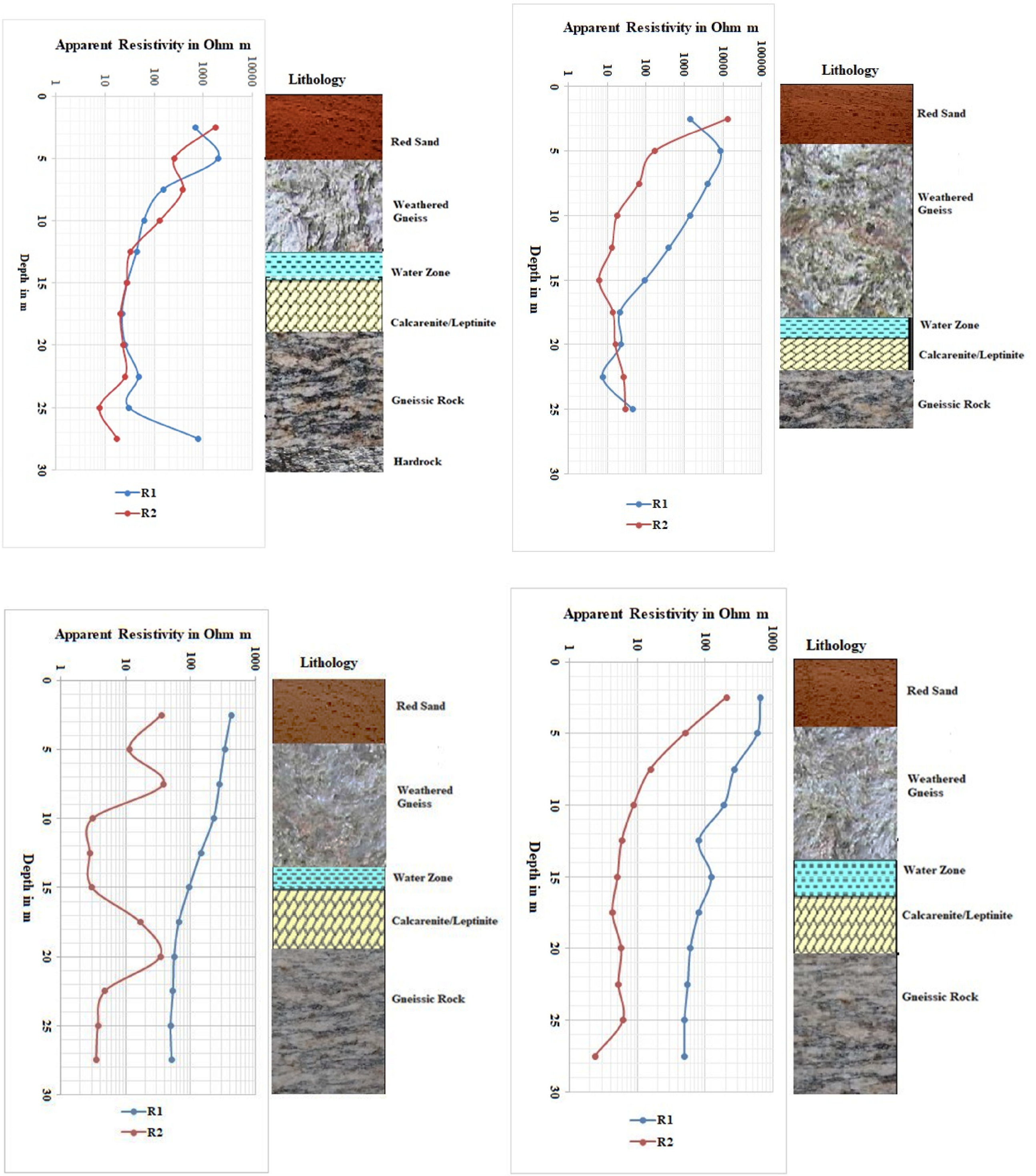

Fig. 4 Electrical resistivity Profile 5 to 8

cations (Ca-Na-Mg) and anions (HCO3-Cl-SO4). The physio-chemical parameters show spatial variation based on sampling location, which indicates influence of local geological controls and geochemical processes on groundwater quality (Mishra et al. 2023). A statistical summary of all groundwater samples provided in Table 2, offering a comprehensive overview of the hydrochemical parameters analysed.

The Piper plot for the 10 samples shows majority falling in the mixed hydrochemical facies region indicating

Table 1 Lithology result from all profiles

Depth from (m)	Depth up to (m)	Formation of Rock	Water identified (yes or no)
0	5	Red soil mix with sand	No
6	12	Weathered gneissic rock	No
13	22	Calcarenite/Leptinite	Yes
23	34	Gneissic rock/some Migmatite rock	No
35	54	Charnockite/pegmatite vein intrusion	Below level

combined influence of rock dominance and evaporation processes (Mussa and Mjemah 2023). Most samples clustered together in the central diamond field except sample A1, which plots separately towards the Ca-Mg-HCO3 end. This indicates that sample A1 has more freshly recharged type composition while other samples represent mixing of different source waters. In general, the samples belong to mixed Ca-Na-HCO3-Cl hydrochemical facies type. This means the ionic composition derived from mixing of different groundwater sources and geochemical reactions like silicate weathering, ion exchange, evaporation etc. (Kuldip-Singh

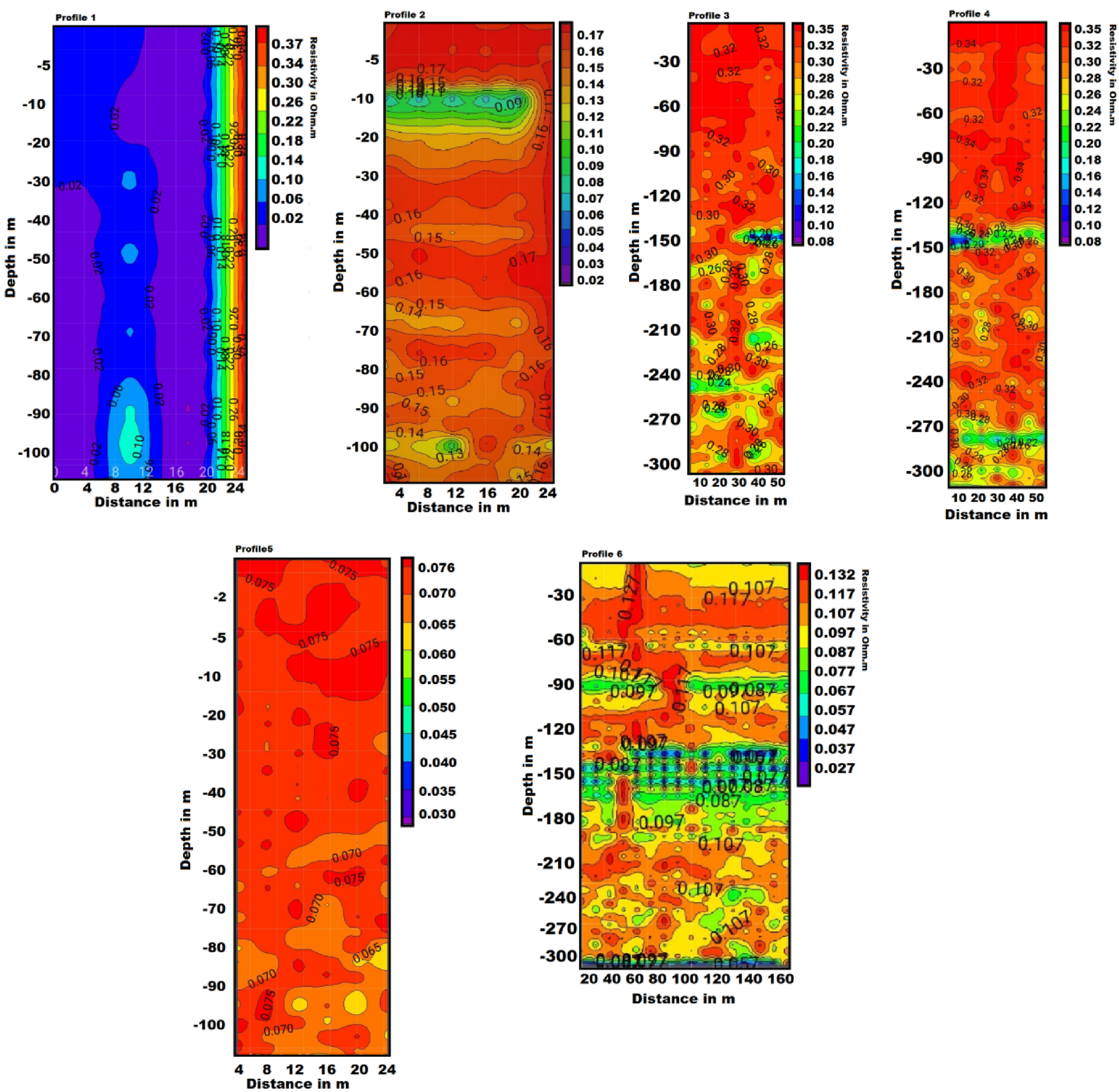

Fig. 5 Magnetotelluric profiles 1 to 6

Table 2 Statistical summary of groundwater samples

Parameter	Unit	Min	Max	Average	St. Dev
pH		6.8	9.7	7.1	7.3
EC	uS/cm	255.0	1070.0	743.0	335.0
TDS	mg/l	170.0	705.0	479.3	209.1
Ca	mg/l	11.0	79.0	58.8	26.5
Mg	mg/l	4.0	23.0	16.9	7.4
Na	mg/l	18.0	94.0	60.6	31.6
K	mg/l	2.0	10.0	6.4	3.4
Fe	mg/l	0.0	0.2	0.0	0.1
Cl	mg/l	31.0	341.0	120.9	89.8
HCO3	mg/l	46.0	295.0	222.7	100.5
SO4	mg/l	7.0	67.0	37.7	24.9

Table 3 Water type of samples collected

Station ID	Latitude	Longitude	Water type
A1	8.294598	77.84691	Ca2 + -Mg2 + -HCO-3-Cl-
A2	8.29018	77.84513	Na + -Ca2 + -HCO-3-Cl-
A3	8.301082	77.83819	Ca2 + -Na + -Cl–HCO-3
A4	8.300565	77.84555	Ca2 + -Na + -Mg2 +—HCO-3-Cl-
A5	8.300174	77.85711	Na + -Ca2 + -Cl–HCO-3
A6	8.311044	77.84691	Ca2 + -Cl—HCO-3
A7	8.309605	77.8481	Na + -Ca2 + -Cl–HCO-3
A8	8.310438	77.84943	Na + -Ca2 + -Cl–HCO-3
A9	8.309809	77.8539	Ca2 + -Na + -Cl–HCO-3
A10	8.309453	77.86518	Na + -Ca2 + -HCO-3-Cl-

et al. 2011). The clustering of most samples in the Piper plot indicates hydrochemical similarities of groundwater from different sampling stations across the study area. This means the major ion chemistry primarily controlled by the geology and geochemical processes, which affect the aquifers in the region (Li et al. 2018). Sample A1 is an outlier possibly due to local recharge source contributing more Ca-HCO3 type signature. Overall, the Piper diagram is indicative of evolutionary history of groundwater as it flows through the aquifer system undergoing different hydro-geochemical processes leading to chemical modifications is shown in Fig. 6 (Table 3).

The Wilcox plot for the samples shows most data points falling in the mixed type water field indicating combined effects of evaporation and rock dominance (Ghalib 2017). One sample falls in the Ca-HCO3 water type region indicating a more freshly recharged composition with low TDS. The other samples distributed along the mixing line that connects

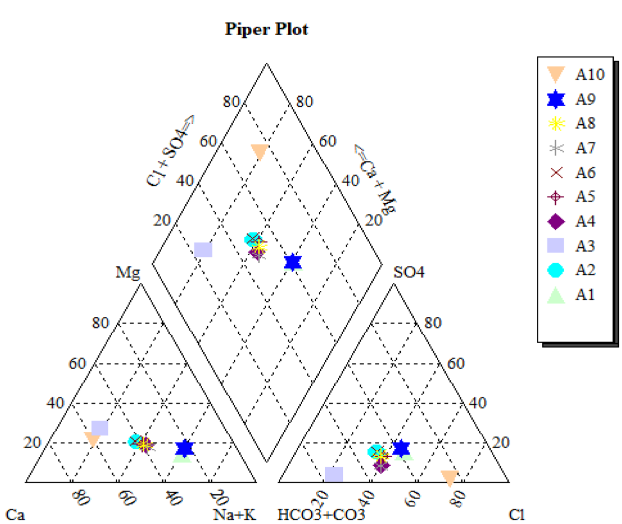

Fig. 6 Piper plot for water samples

Ca2 + dominant waters to Na + K dominant waters, represents base exchange reactions. The samples also align along the mixing line of Cl + SO4 rich waters to HCO3 + CO3 rich compositions indicating influence of evaporation and silicate weathering reactions respectively (Ghalib 2017: Li et al. 2018). Thus, the Wilcox diagram indicates that the samples have evolved through mixing of two end member compositions – a Ca-HCO3 type fresh recharged water and a more mineralized Na-Cl type water. Various hydro-geochemical processes like silicate weathering, base exchange, evaporation and mixing of different source waters across the region results in the mixed composition observed in most samples (Wagh et al. 2018). The Wilcox plot is therefore useful in elucidating the major geochemical processes controlling the ionic compositions and displayed in Fig. 7.

The hydrochemical evolution of the groundwater controlled by several geogenic and anthropogenic factors (Krishna Kumar et al. 2014; Mostafa et al. 2017). In shallow, recently recharged aquifers, the water has a Ca-Mg-HCO3 composition derived from carbonate and silicate mineral weathering. Dissolution of calcite, dolomite and silicate minerals like feldspars releases Ca2 +, Mg2 + and HCO3- ions into the water (Tiwari et al. 2021). Cation exchange of Ca2 + and Mg2 + with Na + on clay minerals can occur (Robin et al. 2015). In deeper, confined aquifers with longer residence times, base exchange of Ca2 + by Na + is more extensive leading to a Na-HCO3 composition (Robin et al. 2015). Upward leakage of deeper Na-HCO3 type water into shallow aquifers can create mixed Ca-Na-HCO3 composition (Do et al. 2020). In areas with longer groundwater flow paths, evaporation leads to concentration of major ions increasing salinity, hardness and shifting the composition towards Na-Cl type (Do et al. 2020). In coastal areas, seawater intrusion due to groundwater over-exploitation introduces more Na + and Cl- ions (Robin et al. 2015; Do et al. 2020). Anthropogenic activities like domestic sewage, agricultural practices and industrial effluents can also provide sources of major ions through water–rock interactions, biochemical

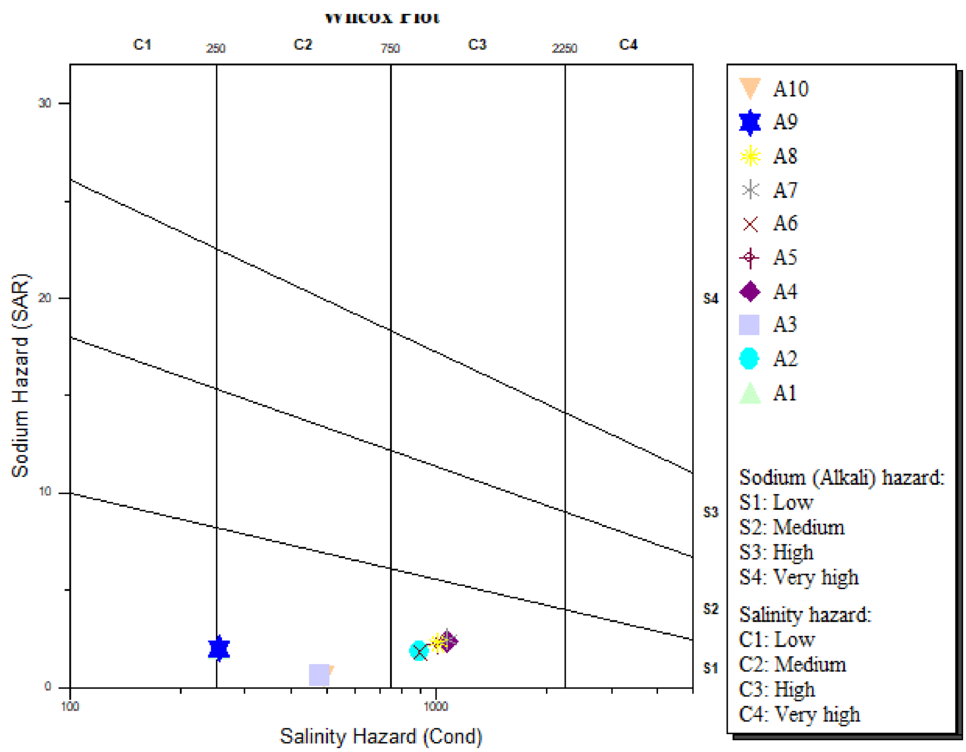

Fig. 7 Wilcox plot for water samples

processes and induced mixing (Krishna Kumar et al. 2014; Mostafa et al. 2017; Nagaraju et al. 2016).

The elevated chloride concentrations found in samples A3, A7, A8 and A9 are interesting anomalies considering the prevailing calcium-rich lithology of weathered gneiss and granitic aquifers in the study area. Typical groundwater chemistry in granite/gneiss terrains is a Ca-Mg-HCO3 water type produced by silicate hydrolysis and carbonate dissolution reactions, which release Ca2 + and HCO3- into solution (Tijani 1994). However, the high chloride and sodium levels in these samples point towards additional sources and processes introducing Na-Cl salts. One possibility is the upward seepage of deeper, confined saline groundwater into the shallow aquifers tapped by these wells (Negm et al. 2018). Cross-formational flow by faults, fractures or breaches identified in the geophysical surveys, creating hydraulic connectivity between deeper and shallow zones. As chloride-rich water intrudes into the shallow calcium-rich aquifer, cation exchange of Ca2 + in clay minerals for Na + from deep water can occur. This base exchange process releases Ca2 + to groundwater but introduces chloride leading to the mixed Ca-Na-Cl composition observed (Raju et al. 2016). The low permeability of the red clayey soil horizons overlying the weathered gneiss can promote longer residence times for groundwater in the subsurface (Comte et al. 2018). Slow seepage of recharge through fine-grained clay-rich soils enhances mineral–water contact and weathering interactions (Comte et al. 2018). Under the suboxic/anoxic conditions in the soils, dissolution of iron hydroxides can release sulfate ions into solution while feldspar hydrolysis may contribute potassium. Longer reaction times associated with sluggish matrix flows in clay zones could potentially contribute to the slightly higher sulphate and potassium noted in sample A5. The fine clays may also impose acidity through associated H + ions (Vaidya and Fogler 1992). However, in areas where the low permeability red soils passed by rapid recharge through fractures, sinkholes and cavities, such chemical effects are likely mitigated. Hence, the red soil influence localized based on predominant flow paths.

High intensity rainfall events during monsoons facilitate large volumes of freshly recharged water rapidly reach the water table through both matrix and preferential flow paths. This dilute younger recharge water flushes the aquifer system, depleting highly soluble ions like chloride while adding calcium released from carbonate dissolution in the unsaturated zone as well as bicarbonate derived from soil zone CO_2 (Ahmed and Clark 2016). In contrast, the dry season has negligible recharge while prolonged residence times and shallow water tables prone to evapotranspiration lead to evaporative concentration of more conservative solutes like chloride and sodium (Ahmed and Clark 2016). Thus, calcium, magnesium and bicarbonate expected to increase after monsoon recharge events while chloride and sodium would be higher in the pre-monsoon summer months. The sampling locations A9 and A10 in the coastal zone provide an opportunity to evaluate potential seawater mixing effects on groundwater chemistry. Interaction between the discharging fresh groundwater and intruding seawater along coastal margins can induce cation exchange, where Ca^{2+} ions in the fresh water exchanged for seawater-derived Na^{+} and Mg^{2+} (Andersen and Nyvang 2020). This promoted calcite dissolution increasing alkalinity and dissolved inorganic carbon. When reduced iron in anoxic groundwater discharges into the toxic seawater environment, rapid oxidation and hydrolysis reactions occur, releasing protons and lowering pH (Ahmed and Clark 2016; Andersen and Nyvang 2020).

Karst identified from magnetotelluric method

The magnetotelluric (MT) and azimuthal square array direct current (DC) electrical resistivity techniques provided complementary geophysical datasets that enabled characterization of the karst aquifer system across multiple depths. While the azimuthal square array method optimized for high resolution shallow profiling to depths of around 40 m, the MT soundings penetrated much greater depths reaching 300 m. This allowed for a comprehensive investigation from the near surface down to the deeper subsurface. The azimuthal square array resistivity results were effective in mapping fractures, weathered zones, and shallow aquifer structures (Habberjam 1972; Ravindran 2012). In contrast, the MT method proved capable of imaging the extensive network of karst conduits, caves and cavities that had developed at varying depths across the study area (Falgàs et al. 2009; Koit et al. 2022). These observed karst features aligned well with the typical stratigraphic patterns expected for limestone and carbonate-dominated aquifer settings. By combining the resistivity and MT datasets, an integrated subsurface model developed delineating the karst formations identified at different depths. This modeling revealed that the shallow karst features mapped by the azimuthal square array method in the depth range of 28–40 m were likely hydrologically connected via deeper conduits to more extensive karst networks imaged by the deeper-penetrating MT method at depths > 150 m. Essentially, the karst structures had coevolved from the near surface down to the deeper subsurface resulting in a complex, interconnected karst drainage system.

The groundwater flow dynamics within this karst drainage system conceptualized based on the observed Geophysical survey and bore hole drilled in Karikovil area depth of around 185 m in the coastal zone. Although the shallow aquifer at Ayankulam appeared saturated, hydraulic gradients showed subsurface flow occurring from this zone to fill the deeper karst conduits. This indicated the prevalence of sinking stream type recharge, where surface water rapidly transmitted through swallow holes, sinkholes and conduits into the deeper karst network. The 2D resistivity-MT model provided visual confirmation of these hypothesized groundwater flow paths connecting the shallow and deep karst structures (Fig. 8).

Conclusion

This integrated study employed electrical resistivity profiling and magnetotelluric surveys along with detailed hydrochemical analysis effectively characterize the complex, multi-layered karst aquifer system in the terrain near Ayankulam village. The electrical resistivity depth soundings identified distinct fractured and weathered zones occurring at shallow depths from 5 to 12 m. These fractured rock layers likely represent perched aquifer units contained within low permeability near-surface clay-rich soils and weathered crust. The resistivity anomalies uncovered at greater depths of 12–22 m probably correspond to leaky confined aquifer formations as well as semi-confined aquifers sandwiched between impermeable layers. The magnetotelluric surveys proved useful in mapping out the extensive network of karst conduits, caves and cavities that have developed in the carbonate formations at varying depths across the study area. These mapped karst structures provide potential preferential flow paths and physical evidence for the downward movement of groundwater from the inland recharge zones near Ayankulam village towards the coast. This groundwater flow connectivity validated by the successful extraction of freshwater from a bore well drilled to a depth of around 185 m in the coastal zone near Karikovil.

The observed Ca-HCO_3 dominated hydrochemical facies along with high dissolved calcium content in the groundwater samples reflects active water–rock interaction and carbonate mineral dissolution processes occurring within the predominant limestone, calcarenite and leptinite lithological formations making up the karst aquifer matrix. The abundance of highly soluble carbonate rocks facilitates rapid chemical weathering reactions as groundwater flows through the aquifer conduits. This results in the dissolution of calcite, dolomite and associated carbonate minerals, leading to the release of Ca^{2+} and HCO_3^- ions into the water. Sinking stream loss identified as the major mechanism for groundwater recharge contributing to the active carbonate dissolution signatures. Spatial variations in recharge sources and geochemical evolution pathways accounted for differences in ionic compositions across the study area. Seasonal changes related to recharge quantities and residence times also caused fluctuations in hydrochemistry. Ultimately, the geochemical and isotopic data coupled with water table contours indicated that excess fresh groundwater draining from the inland recharging karst aquifers discharges into the sea as submarine groundwater discharge. This has implications for freshwater management and indicates potential for exploring mixed Ca-Mg-Na-HCO_3-Cl composition brackish waters for treated utility applications.

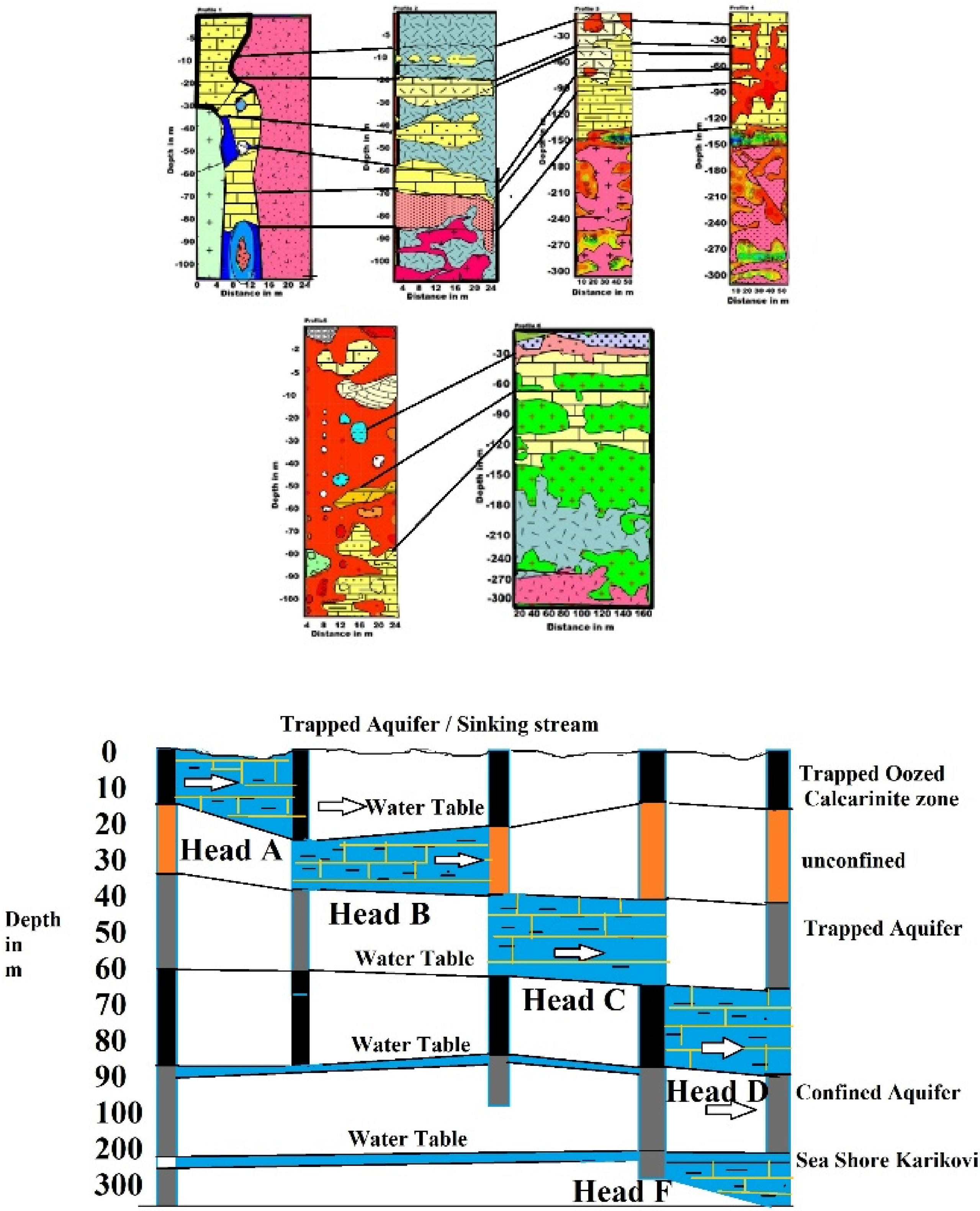

Fig. 8 2D Model prepared from magnetotelluric data compared with existing bore well where water samples collected

Acknowledgements The First author expresses his sincere thanks to Shri. A.P.C.V. Chocka lingam, Secretary and our Principal Dr. C. Veerabhahu, V.O. Chidambaram College, Thoothukudi. Dr. P. Siva Subramanian, Professor and Head, PG and Research Department of Geology, V.O. Chidambaram College, Thoothukudi extended the help.

Author contributions ARA – Supervision and Project administration. AAPA – Conceptualization, Software, Writing – Original Draft and Data Curation. VKJ – Data Collection, Review and Editing. RAS – Data Collection, Review and Editing. ASK – Data Collection and Methodology. AR – Writing – Review & Editing and Methodology. SPR – Writing – Review & Editing.

Funding Not available.

Data availability The datasets generated during and/or analyzed during the current study are available from the corresponding author on reasonable request.

Declarations

Conflicts of interests The authors have no conflicts of interest to declare that are relevant to the content of this article.

Ethics approval Not applicable.

Consent to participate Not applicable.

Consent for publication Not applicable.

References

Abdelzaher, M., Nishijima, J., Saibi, H., El-Qady, G., Massoud, U., Soliman, M., Younis, A., & Ehara, S.: A coastal aquifer study using magnetotelluric and gravity methods in Abo Zenema, Egypt. Pure Appl. Geophys. **169**(9), 1679–1692 (2012). https://doi.org/10.1007/s00024-011-0407-y

Ahmed, A., Clark, I.: Groundwater flow and geochemical evolution in the Central Flinders Ranges, South Australia. Sci. Total Environ. **572**, 837–851 (2016). https://doi.org/10.1016/j.scitotenv.2016.07.123

Albouy, Y., Andrieux, P., Rakotondrasoa, G., Ritz, M., Descloitres, M., Join, J.L., Rasolomanana, E.: Mapping coastal aquifers by joint inversion of DC and TEM soundings-three case histories. Groundwater **39**(1), 87–97 (2001). https://doi.org/10.1111/j.1745-6584.2001.tb00354.x

Andersen, M.S., Nyvang, V.: Coupling of redox processes, calcite dissolution and cation exchange at a fresh-seawater interface in a shallow sandy aquifer. Groundwater **2000**, 225–226 (2020). https://doi.org/10.1201/9781003078593-112

Aris, A.Z., Abdullah, M.H., Kim, K.W.: Hydrogeochemistry of groundwater in Manukan island, Sabah. Mal. J. Anal. Sci. **11**(2), 407–413 (2007)

Bailly-Comte, V., Martin, J.B., Jourde, H., Screaton, E.J., Pistre, S., Langston, A.: Water exchange and pressure transfer between conduits and matrix and their influence on hydrodynamics of two karst aquifers with sinking streams. J. Hydrol. **386**(1–4), 55–66 (2010). https://doi.org/10.1016/j.jhydrol.2010.03.005

Barry, J., Green, J., Rutelonis, J., Steenberg, J., & Alexander, E.: Coupling dye tracing, water chemistry, and passive geophysics to characterize a siliciclastic pseudokarst aquifer, Southeast Minnesota. Proceedings of the 15th Multidisciplinary Conference on Sinkholes and the Engineering and Environmental Impacts of Karst and the 3rd Appalachian Karst Symposium, (2018). https://doi.org/10.5038/9780991000982.1034

Bonacci, O.: Surface waters and groundwater in karst. professional practice in earth sciences, 149–169 (2015). https://doi.org/10.1007/978-3-319-12850-4_5

Bowen, R.:*Groundwater*. Springer Science & Business Media, 1986.

Chou, P.-Y.: The evaluation of deep groundwater recharge in fractured aquifer using distributed fiber-Bragg-grating (FBG) temperature sensors. J. Hydrol. **601**, 126645 (2021). https://doi.org/10.1016/j.jhydrol.2021.126645

Comte, J.-C., Ofterdinger, U., Legchenko, A., Caulfield, J., Cassidy, R., Mézquita González, J.A.: Catchment-scale heterogeneity of flow and storage properties in a weathered/fractured hard rock aquifer from resistivity and magnetic resonance surveys: implications for groundwater flow paths and the distribution of residence times. Geol. Soc. Lond. Special Pub. **479**(1), 35–58 (2018). https://doi.org/10.1144/sp479.11

Demirci, İ, Candansayar, M.E., Vafidis, A., Soupios, P.: Twodimensional joint inversion of direct current resistivity, radio-magnetotelluric and seismic refraction data: an application fromBafra Plain, Turkey. J. Appl. Geophys. **139**, 316–330 (2017). https://doi.org/10.1016/j.jappgeo.2017.03.002

Do, H.-K., Yun, S.-T., Yu, S., Ryuh, Y.-G., Choi, H.-S.: Evaluation of long-term impacts of CO_2 leakage on groundwater quality using hydrochemical data from a natural analogue site in South Korea. Water **12**(5), 1457 (2020). https://doi.org/10.3390/w12051457

Falgàs, E., Ledo, J., Marcuello, A., Queralt, P.: Monitoringfreshwater–seawater inter face dynamics with audiomagnetotelluric data. Near Surf. Geophys. (2009). https://doi.org/10.3997/1873-0604.200903

Ghalib, H.B.: Groundwater chemistry evaluation for drinking and irrigation utilities in east Wasit province, Central Iraq. Appl. Water Sci. **7**(7), 3447–3467 (2017). https://doi.org/10.1007/s13201-017-0575-8

Glynn, P.D., Plummer, L.N.: Geochemistry and the understanding of ground-water systems. Hydrogeol. J. **13**(1), 263–287 (2005). https://doi.org/10.1007/s10040-004-0429-y

Goldscheider, N.: A holistic approach to groundwater protection and ecosystem services in karst terrains. Carbon. Evapor. **34**(4), 1241–1249 (2019). https://doi.org/10.1007/s13146-019-00492-5

Gomo, M.: Use of electric potential difference in audio magnetotelluric (AMT) geophysics for groundwater exploration. Groundw. Sustain. Dev. **20**, 100864 (2023). https://doi.org/10.1016/j.gsd.2022.100864

Habberjam, G.M.: The effects of anisotropy on square array resistivity measurements. Geophys. Prospect. **20**(2), 249–266 (1972). https://doi.org/10.1111/j.1365-2478.1972.tb00631.x

Habberjam, G.M., Watkins, G.E.: The use of a square configuration in resistivity prospecting. Geophys. Prospect. **15**(3), 445–467 (1967a). https://doi.org/10.1111/j.1365-2478.1967.tb01798.x

Habberjam, G.M., Watkins, G.E.: The reduction of lateral effects in resistivity probing. Geophys. Prospect. **15**(2), 221–235 (1967b). https://doi.org/10.1111/j.1365-2478.1967.tb01785.x

Jeelani, G., Bhat, N.A., Shivanna, K., Bhat, M.Y.: Geochemical characterization of surface water and spring water in SE Kashmir Valley, western Himalaya: Implications to water–rock interaction. J. Earth Syst. Sci. **120**(5), 921–932 (2011). https://doi.org/10.1007/s12040-011-0107-0

Katz, B.G., Catches, J.S., Bullen, T.D., Michel, R.L.: Changes in the isotopic and chemical composition of ground water resulting from a recharge pulse from a sinking stream. J. Hydrol. **211**(1–4), 178–207 (1998). https://doi.org/10.1016/s0022-1694(98)00236-4

Kaufmann, G., Romanov, D.: Structure and evolution of collapse sinkholes: combined interpretation from physico-chemical modelling and geophysical field work. J. Hydrol. **540**, 688–698 (2016). https://doi.org/10.1016/j.jhydrol.2016.06.050

Khan, R., Jhariya, D.C.: Hydrogeochemistry and groundwater quality assessment for drinking and irrigation purpose of Raipur City, Chhattisgarh. J. Geol. Soc. India **91**(4), 475–482 (2018)

Koit, O., Mayaud, C., Kogovšek, B., Vainu, M., Terasmaa, J., Marandi, A.: Surface water and groundwater hydraulics of lowland karst aquifers of Estonia. J. Hydrol. **610**, 127908, (2022). https://doi.org/10.13140/RG.2.2.13634.86726

Krishna Kumar, S., Bharani, R., Magesh, N.S., Godson, P.S., Chandrasekar, N.: Hydrogeochemistry and groundwater quality appraisal of part of south Chennai coastal aquifers, Tamil Nadu, India using WQI and fuzzy logic method. Appl. Water Sci. **4**(4), 341–350 (2014)

Lane, J.W., Jr., Haeni, F.P., Watson, W.M.: Use of a square-array direct-current resistivity method to detect fractures in crystalline bedrock in New Hampshire. Groundwater **33**(3), 476–485 (1995). https://doi.org/10.1111/j.1745-6584.1995.tb00304.x

Li, J., Pang, Z., Kong, Y., Lin, F., Wang, Y., Wang, G., Lv, L.: An integrated magnetotelluric and gamma exploration of groundwater in fractured granite for small-scale freshwater supply: a case study from the Boshan region, Shandong Province, China. Environ. Earth Sci. **76**(4), 1–12 (2017). https://doi.org/10.1007/s12665-017-6486-z

Li, X., Wu, H., Qian, H., Gao, Y.: Groundwater chemistry regulated by hydrochemical processes and geological structures: a case study in Tongchuan, China. Water **10**(3), 338 (2018). https://doi.org/10.3390/w10030338

Martel, R., Castellazzi, P., Gloaguen, E., Trépanier, L., Garfias, J.: ERT, GPR, InSAR, and tracer tests to characterize karst aquifer systems under urban areas: the case of Quebec City. Geomorphology **310**, 45–56 (2018). https://doi.org/10.1016/j.geomorph.2018.03.003

Miao, Z., Carroll, K.C., Brusseau, M.L.: Characterization and quantification of groundwater sulfate sources at a mining site in an arid climate: the Monument Valley site in Arizona, USA. J. Hydrol. **504**, 207–215 (2013). https://doi.org/10.1016/j.jhydrol.2013.09.030

Mishra, A., Rai, A., Mishra, P.K., Rai, S.C.: Evaluation of hydrochemistry in a phreatic aquifer in the Vindhyan Region, India, using entropy weighted approach and geochemical modelling. Acta Geochimica **42**(4), 648–672 (2023). https://doi.org/10.1007/s11631-023-00610-0

Mostafa, M.G., Uddin, S.M., Haque, A.B.M.H.: Assessment of hydrogeochemistry and groundwater quality of Rajshahi City in Bangladesh. Appl. Water Sci. **7**(8), 4663–4671 (2017)

Nagaraju, A., Muralidhar, P., Sreedhar, Y.: Hydrogeochemistry and groundwater quality assessment of Rapur area, Andhra Pradesh, South India. J. Geosci. Environ. Prot. **4**(4), 88–99 (2016)

Negm, A.M., Sakr, S., Abd-Elaty, I., Abd-Elhamid, H.F.: An overview of groundwater resources in Nile Delta aquifer. Groundwater in the Nile Delta, 3–44, (2018). https://doi.org/10.1007/698_2017_193

Nenna, V., Herckenrath, D., Knight, R., Odlum, N., McPhee, D.: Application and evaluation of electromagnetic methods for imaging saltwater intrusion in coastal aquifers: Seaside Groundwater Basin, California. Geophysics **78**(2), B77–B88 (2013). https://doi.org/10.1190/geo2012-0004.1

Obiadi, I.I., Onwuemesi, A.G., Anike, O.L., Ajaegwu, N.E., Anakwuba, E.K., Nwosu, C.M., et al.: Determining subsurface fracture characteristics from the azimuthal square array resistivity survey at Igarra, Nigeria. Pure Appl. Geophys. **170**(5), 907–916 (2013). https://doi.org/10.1007/s00024-011-0443-7

Raju, N.J., Patel, P., Reddy, B.C.S.R., Suresh, U., Reddy, T.V.K.: Identifying source and evaluation of hydrogeochemical processes in the hard rock aquifer system: geostatistical analysis and geochemical modeling techniques. Environ. Earth Sci. **75**(16), 1 (2016). https://doi.org/10.1007/s12665-016-5979-5

Ramanujam, N., Murugan, K.N., Ravindran, A.A.: Azimuthal square array resistivity studies to infer active fault zones in the areas of known seismicity, Kottayam district, Kerala: a case study. J. Ind. Geophys. Union **10**(3), 197–208 (2006)

Ravindran, A.A.: Azimuthal square array method and groundwater potential zone in hard rock area in Thoothukudi District, Tamilnadu. Arch. Appl. Sci. Res. **4**(2), 971–979 (2012)

Robin, V., Tertre, E., Beaufort, D., Regnault, O., Sardini, P., Descostes, M.: Ion exchange reactions of major inorganic cations (H+, Na+, Ca2+, Mg2+ and K+) on beidellite: experimental results and new thermodynamic database. Toward a better prediction of contaminant mobility in natural environments. Appl. Geochem. **59**, 74–84 (2015). https://doi.org/10.1016/j.apgeochem.2015.03.016

Şener, A., Pekşen, E., Yolcubal, İ: Application of square array configuration and electrical resistivity tomography for characterization of the recharge area of a karst aquifer: a case study from Menekşe karst plateau (Kocaeli, Turkey). J. Appl. Geophys. **195**, 104474 (2021). https://doi.org/10.1016/j.jappgeo.2021.104474

Singh, K., Hundal, K., Singh, D.: Geochemistry and assessment of hydrogeochemical processes in groundwater in the southern part of Bathinda district of Punjab, northwest India. Environ. Earth Sci. **64**(7), 1823–1833 (2011). https://doi.org/10.1007/s12665-011-0989-9

Tijani, M.N.: Hydrogeochemical assessment of groundwater in Moro area, Kwara state, Nigeria. Environ. Geol. **24**(3), 194–202 (1994). https://doi.org/10.1007/bf00766889

Tiwari, A.K., Singh, A.K., Giri, S., Mahato, M.K.: Major ion chemistry and hydrochemical processes controlling water composition of Teesta River catchment, Sikkim Himalaya, India. Int. J. Environ. Anal. Chem. **103**(20), 8597–8615 (2021). https://doi.org/10.1080/03067319.2021.1992402

Vaidya, R.N., Fogler, H.S.: Fines migration and formation damage: influence of pH and ion exchange. SPE Prod. Eng. **7**(04), 325–330 (1992). https://doi.org/10.2118/19413-pa

Vozoff, K.: The magnetotelluric method. (1991). https://doi.org/10.1190/1.9781560802686.ch8

Wagh, V.M., Panaskar, D.B., Jacobs, J.A., Mukate, S.V., Muley, A.A., Kadam, A.K.: Influence of hydro-geochemical processes on groundwater quality through geostatistical techniques in Kadava River basin, Western India. Arab. J. Geosci. **12**, 1 (2018). https://doi.org/10.1007/s12517-018-4136-8

White, W.B.: Karst hydrology: recent developments and open questions. Eng. Geol. **65**(2–3), 85–105 (2002). https://doi.org/10.1016/s0013-7952(01)00116-8

Xiao, J., Jin, Z.D., Wang, J., Zhang, F.: Hydrochemical characteristics, controlling factors and solute sources of groundwater within the Tarim River Basin in the extreme arid region, NW Tibetan Plateau. Quatern. Int. **380–381**, 237–246 (2015). https://doi.org/10.1016/j.quaint.2015.01.021

Yeboah-Forson, A., Whitman, D.: Electrical resistivity characterization of anisotropy in the Biscayne aquifer. Groundwater **52**(5), 728–736, (2013). Portico. https://doi.org/10.1111/gwat.12107

Zhu, J., Currens, J.C., Dinger, J.S.: Challenges of using electrical resistivity method to locate karst conduits—a field case in the Inner Bluegrass Region, Kentucky. J. Appl. Geophys. **75**(3), 523–530 (2011). https://doi.org/10.1016/j.jappgeo.2011.08.009